

MOK3: a High Field Magneto-Optical Kerr probe

User Manual

Wilhelmus J. Geerts
National High Magnetic Field Laboratory
Gainesville / Tallahassee
Friday, July 25, 1997

This probe was designed at the University of Florida and developed into a user facility at the National High Magnetic Field Laboratory in Tallahassee. The work was done under supervision of:

Dr. Bruce L. Brandt

Prof. Dr. Jeffrey R. Childress

Prof. Dr. Steve J. Pearton

Abstract: This manual describes MOK3, a Magneto-Optical “Kerr”¹ probe (prototype 3) to be used in the 50 mm bore magnets of the NHMFL in Tallahassee. MOK3 can be used to do Magneto-Optical measurements on thin films, transparent materials, liquids, and gasses in fields up to 20 tesla (in the near future 25 tesla) and at temperatures of 2K to 325K. Typical sample diameters are between 0.5 cm and 2 cm. MOK3 has a rotation noise level of less than 0.5 mdegree on bulk iron, and a residual system background smaller than 2 mdegree/tesla. A better signal to noise ratio and a lower system background is obtained for the ellipticity signal.

The light source of MOK3 is a HeNe laser (632 nm). The wavelength window of the optics is 325 - 1600 nm. Although other cylindrical (external power supply) lasers can be used in MOK3, the laser light source can NOT be replaced by a lamp.

The equipment, the first in its kind, was designed to be as multifunctional as possible. Its modular structure allows modifications and the insertion of user-dependent sample holders. For those users interested in designing their own sampleholder a technical report is available which includes a service manual, design rules and reasons, addresses, references, and the technical drawings. The report can be requested from the Director of Operation, Dr. Bruce Brandt, 1800 E. Paul Dirac Dr., Tallahassee.

Tallahassee 7-27-97.

¹ In memory of the Scottish physicist John Kerr [Kэ:], 1824-1907 [1].

Contents:

Abstract

Contents

0 Introduction

1. Experimental Setup:

1.1 Description of the Magneto-Optical Probe

1.1.1 The lower course

1.1.2 The upper course

1.1.3 The vacuum jacket

1.2 Electronic Equipment

1.2.1 Description

1.2.2 Settings of the equipment

1.3 Data acquisition

1.4 Cryogenics

1.5 Vacuum and magnetic shielding

2 Background information:

2.1 Measurement technique

2.2 Calibration

2.3 Specifications

2.4 Trouble shooting list “UNDER CONSTRUCTION”

References.

0. Introduction.

Magneto-Optical (MO) effects arise from an optical anisotropy which changes the polarization state of incident linearly polarized light into rotated elliptically polarized light after reflection from or transmission through a material (see Fig. 0.1). The former we call the MO Kerr effect [1], and the latter is called the MO Faraday effect [2]. In reflection mode, one distinguishes between three Kerr effects, depending on the relative orientation of the magnetization M with respect to the plane of incidence of the light (see Fig 0.2): the polar, the longitudinal and transverse Kerr effect [3].

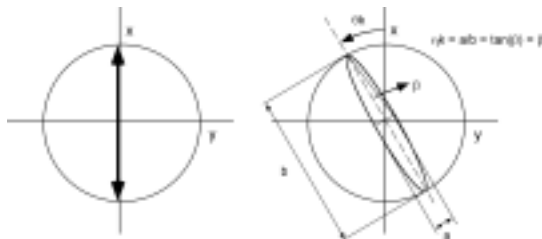


Figure Error! No text of specified style in document.-1: State of Polarization of incident beam (left) and reflected beam (right).

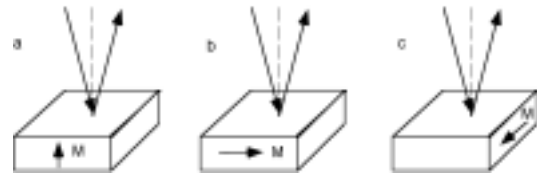


Figure Error! No text of specified style in document.-2: The three Kerr configurations: (a) Polar, (b) Longitudinal, (c) Transverse

The MO effects originate from a combination of exchange interaction or bandsplitting by an externally applied magnetic field, and spin orbit interaction. From quantum mechanics it follows that optical transitions are not allowed between all bands or energy levels. For

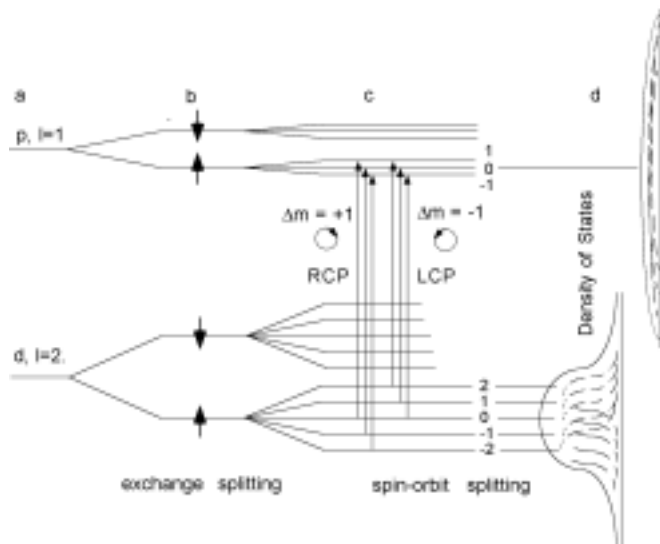


Figure Error! No text of specified style in document.-3: Microscopic origin of the MO effects: simplified energy-level scheme for a transition: (a) fully degenerate, (b) including exchange splitting, (c) including spin-orbit interaction, (d) in a material with a bandstructure.

this reason the material will have different absorption coefficients and refraction indices for Right Circular Polarized light (RCP) and Left Circular Polarized light (LCP). The circular dichroism causes the reflected or transmitted beam to be slightly elliptically polarized. The circular birefringence causes the small rotation of the polarization plane. Fig. 0.3 gives a simplified energy-level scheme [3]. A more extensive overview of the MO effects of solids can be found in [6-10].

For homogeneous ferromagnetic materials, the magneto-optical effects, can be considered to be linear with magnetization [5]. So by measuring the rotation or ellipticity changes as a function of the field one can probe the magnetic hysteresis curve, in certain respect the fingerprint of the material. When used on materials with a large absorption coefficient the technique is very surface sensitive. The Kerr signal stems only from about twice the penetration depth of the light, d_p , for which the intensity of the light is reduced to $1/e$:

$$d_p = \frac{\lambda}{4\pi k}$$

where λ is the wavelength and k the absorption coefficient. d_p is typically about 15-30 nm for metals in the visible wavelength range. This makes the technique very surface sensitive, and very suitable for the study of ultrathin films. Iron films in the sub-atomic layer range can be successfully studied by this technique. Table 1 gives an overview of the other magnetometers which are available at NHMFL.

Table 1: High field magnetometers.

Method	Conditions	Sensitivity
Lakeshore VSM probe	33 tesla, 0.5 .. 350 K	10^{-3} emu
Lakeshore AC susceptometer	33 tesla, 20 mK .. 350 K	10^{-4} emu
Cantilever Beam Magnetometer	33 tesla, 20 mK .. 350 K	$10^{-7} \dots 10^{-9}$ emu
Kerr Magnetometer	20 tesla, 2 .. 300 K	$10^{-9} \dots 10^{-10}$ emu
Oscillating Reed Magnetometer		$10^{-11} \dots 10^{-12}$ emu

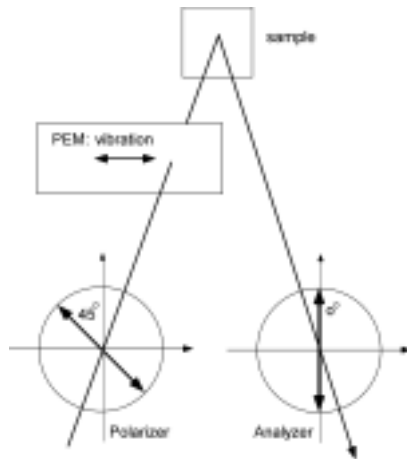


Figure Error! No text of specified style in document.-4: Global Measurement scheme.

The measurement technique applied in MOK3 is based on the photo-elastic modulator technique. A Photo-elastic modulator (PEM) consists of a birefringent crystal (e.g. SiO₂) which is sinusoidally expanded and contracted in one direction by a piezo-electric actuator. Linear polarized waves with a polarization plane parallel to this direction are retarded when the element is expanded, and advanced when it is contracted. In this way a periodically varying phase shift is added. Linear polarized waves with a plane of polarization orthogonal to the contraction direction are not influenced. The modulation frequency typically is 50 kHz. Originally this detection scheme was used for spectroscopic

measurements of the complex index of refraction [11], but with minor changes the detection scheme is suited for Kerr rotation and ellipticity measurements [12,4]. The

global measurement scheme of MOK3 is given in figure 0.4. The light leaving the polarizer/modulator unit will change between RCP and LCP light with a frequency of 50 kHz. A small rotation or ellipticity introduced by the sample will result in the occurrence of respectively 2ω and 1ω signals (see Fig. 0.5). The exact change of the State Of Polarization (SOP) of the beam can be derived from those signals. A more detailed explanation of the measurement technique can be found in section 2.1.

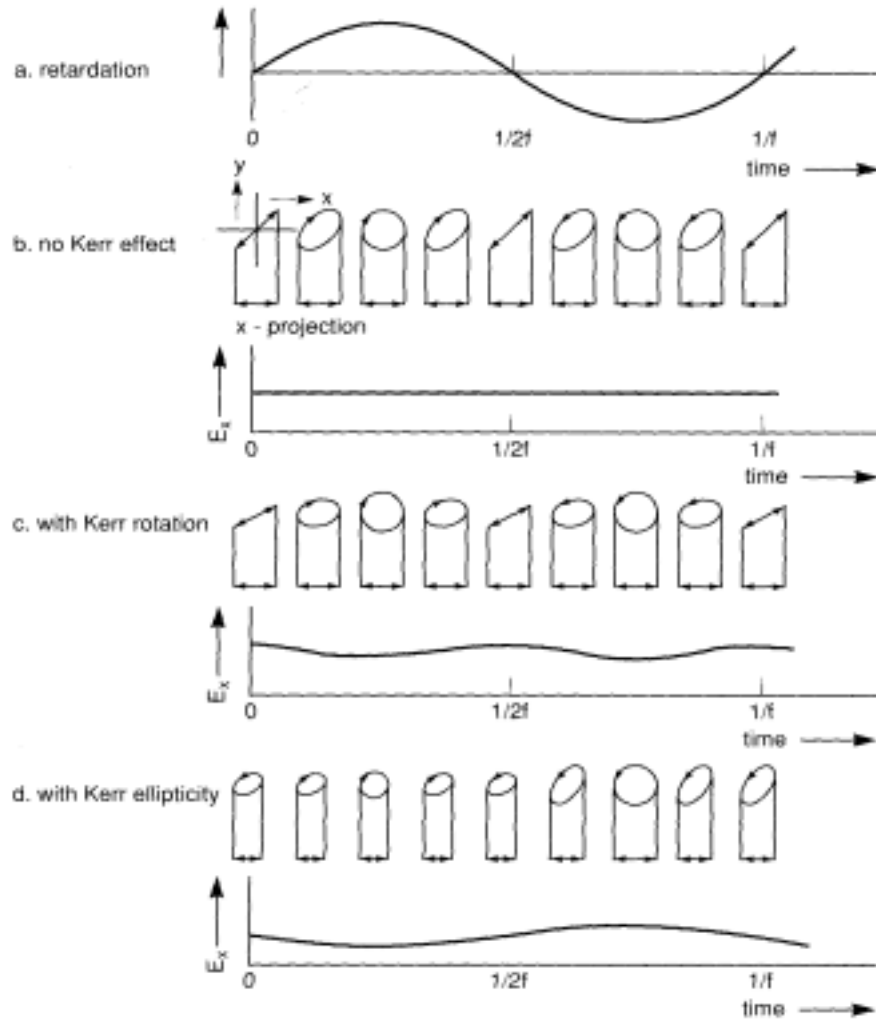


Figure Error! No text of specified style in document.-5: (a) retardation of the PEM as a function of the time, (b) polarization state of corresponding light vector, (c) as (b) but after introduction of Kerr rotation, (d) as (b) but after introduction of Kerr ellipticity [12]

1. Experimental setup

1.1 Description of the Magneto-Optical Probe.

The Magneto-Optical probe consists of a long stainless steel tube of 2 meters (lower course) with the optics (upper course) mounted on top of it. The lower course fits in a vacuum jacket which can be evacuated in order to allow measurements at low temperature. Other reasons to evacuate the lower course is to increase the mechanical stability and to avoid large Kerr rotation contributions of the air in the light path (≈ 22 mdegree/tesla).

1.1.1 The lower course.

The lower course consists of (from top to bottom) the shielded vacuum window, the shielded lens unit, the constrictor, the sample stage, and the center unit (Fig. 1.1-3). The center unit and the constrictor are included in the final design to improve the mechanical stability of the probe. They support the probe in the vacuum jacket and guarantee that the assembled setup has sufficient rigidity. More about these in section 1.1.3.

The sample stage consists of a round table of 20 mm diameter which can be tilted with respect to the XY-plane by two manipulation rods (see Fig. 1.2). This is necessary in order to align the beam which is reflected from the sample. The tilting stage contains a Cernox temperature sensor and a 50 ohm heater coil. Sensor (4 wires) and heater (2 wires) are connected to a standard 19 pins Detoronix connector via a vacuum feedthrough in the vacuum window unit.

There are four different measurement configurations, i.e. polar Kerr, longitudinal Kerr, and polar Faraday mode. In the polar Kerr configuration, the sample is mounted directly on the table by varnish, or a brass spring. A tight sample mounting is crucial for good results. Preferably one should use the tapered shaped copper ring (see Fig. 1.2a) so that only light which reflects from the sample will be able to find its way up through the lower course of the probe. For measurements in the polar Faraday mode the special adapter of Fig. 1.2b is proposed. The light propagates through the sample, is



Figure 1.1: lower course probe.

reflected from a mirror, and propagates again through the sample. Figure 1.2c shows an adapter which can be used in order to do Longitudinal Kerr measurements (i.e. parallel to the film surface): the incident beam is reflected off the input mirror, hits the sample at an angle of 45 degrees and reflects off the output mirror.

Above the table is a space of at least 2.5 cm . This should provide sufficient space for a diamond anvil cell, a quartz glass cell for measurements on liquids or gasses, or many other interesting applications.

The shielded lens unit, in the middle of the lower course, contains a lens with a focal length of 1 meter. The lens is used to focus the laser beam on the sample.

The shielded vacuum window unit at the top of the lower course contains the mechanical and electrical feedthroughs and acts as a base for the upper course of the probe.

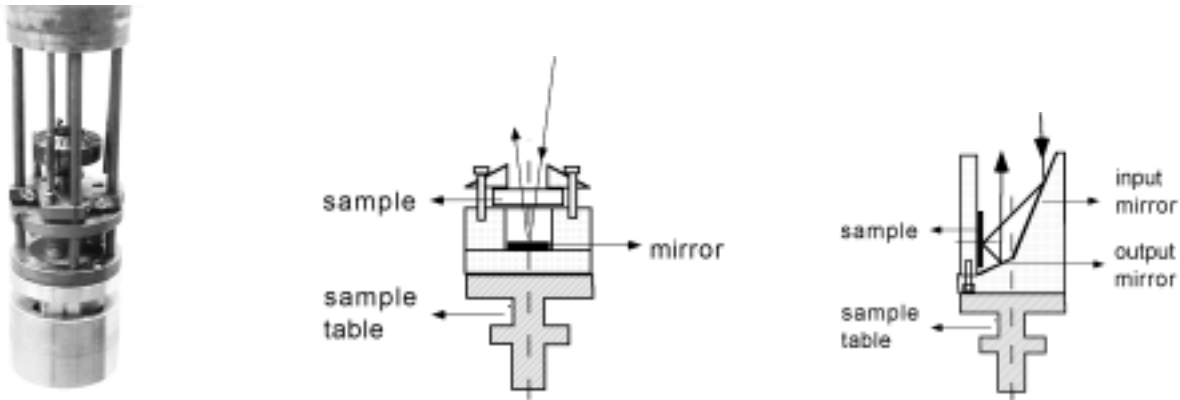


Fig. 1.2: (a) sample stage close up, (b) Faraday adapter, (c) Longitudinal adapter

1.1.2. The upper course.

The upper course of the probe (see Fig. 1.3), is mounted by brass screws and aluminum spacers on the top of the lower course. It consists of the laser platform, the polarizer/modulator holder, the deflection unit and the analyzer/detector holder.

The laser platform contains a linear polarized HeNe laser of 2 mW and a deflection mirror. The deflection mirror is mounted on a tilting stage that allows one to line up the incident beam parallel to the probe.

The shielded Polarizer/Modulator holder contains a Hinds Photo-elastic modulator (fused silica, 50 kHz) and a Glan-Thompson polarizer. The angle between the polarization plane of the polarizer and the modulation direction of the PEM is set at 45 degrees (see also Fig. 0.4).

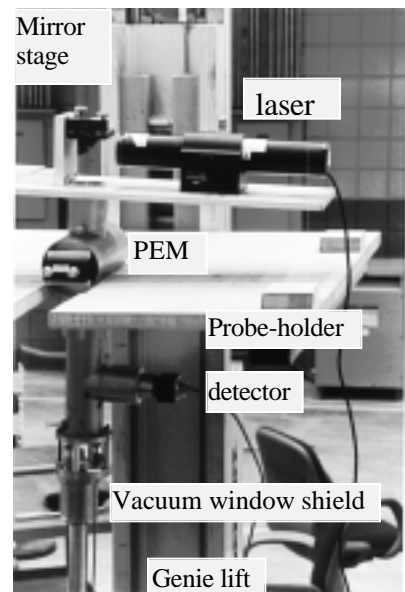


Figure1.3: upper course

This angle should not be changed by the user without asking the responsible NHMFL staff person (it can change the calibration of the probe).

The whole unit can be rotated about its axis. A slight angle between the k-vector and the modulators normal is recommended as it avoids interference effects in the modulator [13]. The deflection unit is used to separate the incident and reflected beam. Both beams propagate more or less anti-parallel in the upper course of the probe and are separated by approximately 12 mm. The mirror unit consists of two aluminum mirrors. Both reflections are 45 degrees (s-component of first mirror is p-component of second mirror and the other way around). The optical transfer function of the deflection unit is the unity matrix: i.e. the mirror unit does not change the SOP of the light passing through it. The Glan-laser polarizer in the analyzer/detector module is shielded. It can be rotated freely over 360 degrees. The light passing through the analyzer is focused on a detector by a lens with a focal length of 1 inch. The detector is an amplified silicon detector.

1.1.3 The Vacuum jacket

The vacuum jacket is a stainless steel tube construction. It consists of a 2 inch diameter stainless steel tube at the top, and a 1.5 inch diameter tail. The latter fits in the tail of the cryostats. The vacuum jacket fits over the lower course of the probe. The probe is supported on three points in the vacuum jacket in order to guarantee a maximum rigidity. At the top by a quikfitting around the vacuum window shield, at the beginning of the tail by the

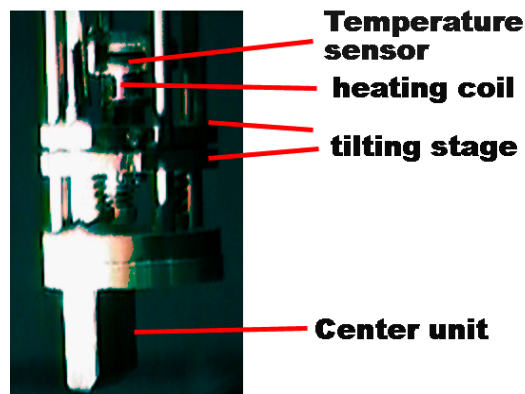


Figure 1.4: Center unit

constrictor (a locking wedge of 3 degrees), and at the bottom of the tail by the center unit. The center unit is an off-centered tapered pin at the end of the sample stage (see Fig. 1.4) which fits in a congruent hole in the bottom of the vacuum jacket. Figure 1.2.a gives both, the pin and the cylinder with the congruent hole in it. The center unit is spring driven and allows vertical movements but forbids any movements in a horizontal plane. (see Fig. 1.4 and Fig. 1.2.a). When inserting the probe into the vacuum jacket the orange dots on probe and vacuum jacket should line up so that center unit and constrictor can lock up.

1.1.4 Optical alignment.

The alignment strategy for the polar and longitudinal configuration are given in Fig. 1.5a and Fig. 1.5b. The alignment procedure for the polar configuration will be outlined below. Alignment is necessary in order to obtain a good signal to noise ratio and in order to be sure that the reflected beam caught by the detector originates from the sample. For a good signal to noise ratio, it is crucial that the beam nowhere touches the probe (i.e. parts of the probe should not act like a diaphragm). The high pressure cooling water circuit of the magnet causes the probe to vibrate slightly with a frequency of 10-1000 Hz which will result in small vibrations in the light path. In the case that some of the parts act as a diaphragm, these vibrations will result in large intensity variations.

For the polar configuration, in the upper part of the probe both beams are anti-parallel and separated by 12 mm (see Fig. 1.5a). The lens will focus the beam on the sample (beam diameter 2 mm). For alignment procedures a standard Genie lift equipped with a wooden probe-holder is used. The probe should be shifted with its PEM holder in the 2.2 inch slit (see Fig. 1.3). Do not hook the probe behind its laser plateau, as this is not strong enough, will bend, and will misalign the beam after removing the probe from the lift.

The alignment procedure is done in two phases. First we have to align the incident beam and then we have to align the reflected beam.

The incident beam can be aligned with the mirror-tilting stage on the laser platform. Two tilting screws give the opportunity to tilt the beam. One revolution of the tilting screws will shift the focused beam at the sample over approximately 10 mm. Only slight corrections for the tilting angle are necessary after loading in a new sample.

A more rigorous alignment has to be done each time you remove the laser. To ease this procedure a special alignment elbow has been constructed. When two of the aluminum distance spacers are removed between upper and lower course, the elbow can be shifted in (Fig. 1.6). When the incident beam goes through the middle of the iris on top of the laser platform and through the marked hole in the alignment elbow it will almost surely hit the sample.

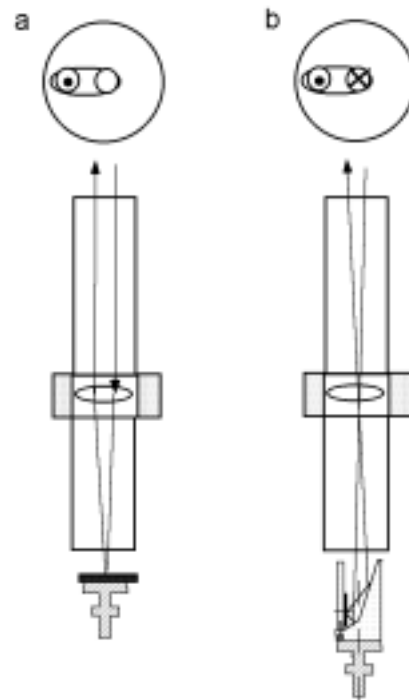


Figure 1.5 : alignment strategy for (a) polar configuration, (b) longitudinal configuration.

The reflected beam has to be aligned by using the alignment rods, which can be accessed on the top of the lower course. This alignment is more sensitive than the adjustment for the incident beam. The reflected beam has to come back through the large hole in the elbow. Remove the analyzer/detector unit and check if the beam hits the edges of one of the two mirrors. In the case of small Kerr rotation and Kerr ellipticity values (<10 mdegree), one should be sure that both reflections are 45 degrees and that the beam neatly lines up with the axis of the analyzer.

The best way to insert the probe in the vacuum jacket, is to remove it from the probe-holder and to lay it on the floor. First remove the cables connected to the probe. **Short-circuit** the contacts of the laser connector on the probe to remove residual electric charge and thus to avoid nasty shocks. When shifting the probe into the vacuum jacket be sure that the orange dots on Quik-fitting and vacuum window unit correspond in order to be sure that the tapered pin at the bottom of the probe shifts into the spring driven center unit. The center unit and the constrictor can be locked by positioning the probe and vacuum jacket vertical.

Do not rotate the probe over large angles with respect to the vacuum jacket once the whole assembly is positioned vertically. It might damage the center unit at the bottom of the vacuum jacket.

Once locked, the probe has to be evacuated. The 250 Newton of the vacuum and the weight of the probe will guarantee sufficient mechanical stability.

The whole alignment procedure will take somewhere between 10 and 20 minutes depending on the experience and initial configuration.

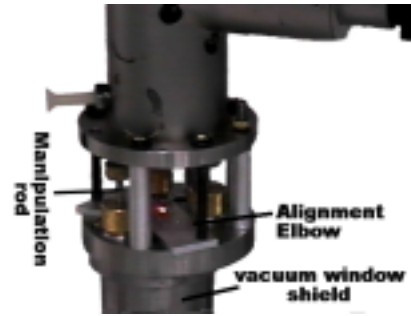


Figure 1.6: alignment elbow

1.2 Electronic Equipment.

1.2.1 Description.

The necessary electronic connections are given in Fig. 1.7. The PEM modulator consists of four different parts; the controller, the electronic head, the special BNC cables, and the optical head.

Never operate the controller when the optical head is not connected as this will damage the equipment.

The electronic head is very sensitive to magnetic fields and should be kept away from the magnet as far as possible. The special BNC cables are matched with the electronic and optical head and may only be used for the Magneto-Optical setup. After finishing your experiments please keep them with the probe in cell 1a (do not bring them to the instrument shop because when they are lost the equipment becomes useless). The same remark has to be made for the power cable of the silicon amplifier detector and the laser extension cable.

The detector signal is connected via a normal BNC cable and the 50 ohm impedance match to the signal conditioning unit of HINDS instruments. This is a broad band amplifier. The amplification factor of the dc signal and the ac signal can be set separately.

Do not change its settings without telling the responsible staff person of NHMFL, as the calibration of the system depends on it (see also chapter 2).

The AC-signal output is connected to two Stanford SR830 lock-in amplifiers. One for the 1ω component (ellipticity) and the other for the 2ω component (rotation). In order to get rid of the laser noise and small intensity variations caused by the movement of the reflected beam, the AC signals have to be divided by the DC signal: the DC-output of the HINDS signal conditioner is connected to the AUXin1 inputs on the rear side of the lock-in amplifiers.

Both Lock-in amplifiers are connected via a GPIB cable to a data-acquisition system. The working of the temperature controller, the LTC-20 of Conductus, is straight forward. See the manual of that specific apparatus.

1.2.2. Settings of the equipment.

Best results are obtained if the dc-signal of the HINDS signal conditioner is somewhere between 1 and 10 volt. If the signal becomes lower because of the high absorption in the sample, it is better to increase the gain of the amplifier-detector. This will not influence the calibration of the instrument. Another way to change the intensity is to rotate the laser tube: lining it up with the polarization plane of the polarizer will increase the signal, while rotating it away from it will decrease the signal. Be aware that rotating the laser tube might make realignment necessary. Be sure that both the silicon amplifier detector and the Hinds signal conditioner do not saturate.

The angle between the polarization plane of the analyzer and the modulator direction is normally set at 0 (in MOK3 horizontally). Fine adjustment can be obtained by monitoring the detector signal on a scope and minimizing the AC signal. Best results are obtained by rotating the analyzer 1-2 degrees from this minimum.

Typical settings of the lock-in amplifiers are given below:

ONE- ω signal: 300 mseconds, 500 mvolt, A input, 18 dB filter, Harm1, ratio AUX1, X-signal, pos. edge, display, AC, float.

TWO- ω signal: similar but Harm2 instead of Harm1.

The time-constant of the Hinds signal conditioner should be set equal to those of the lock-in amplifiers. A time constant of 300 mseconds should allow you to sweep field with a speed of 100 Amp/second without introducing electronic hysteresis.

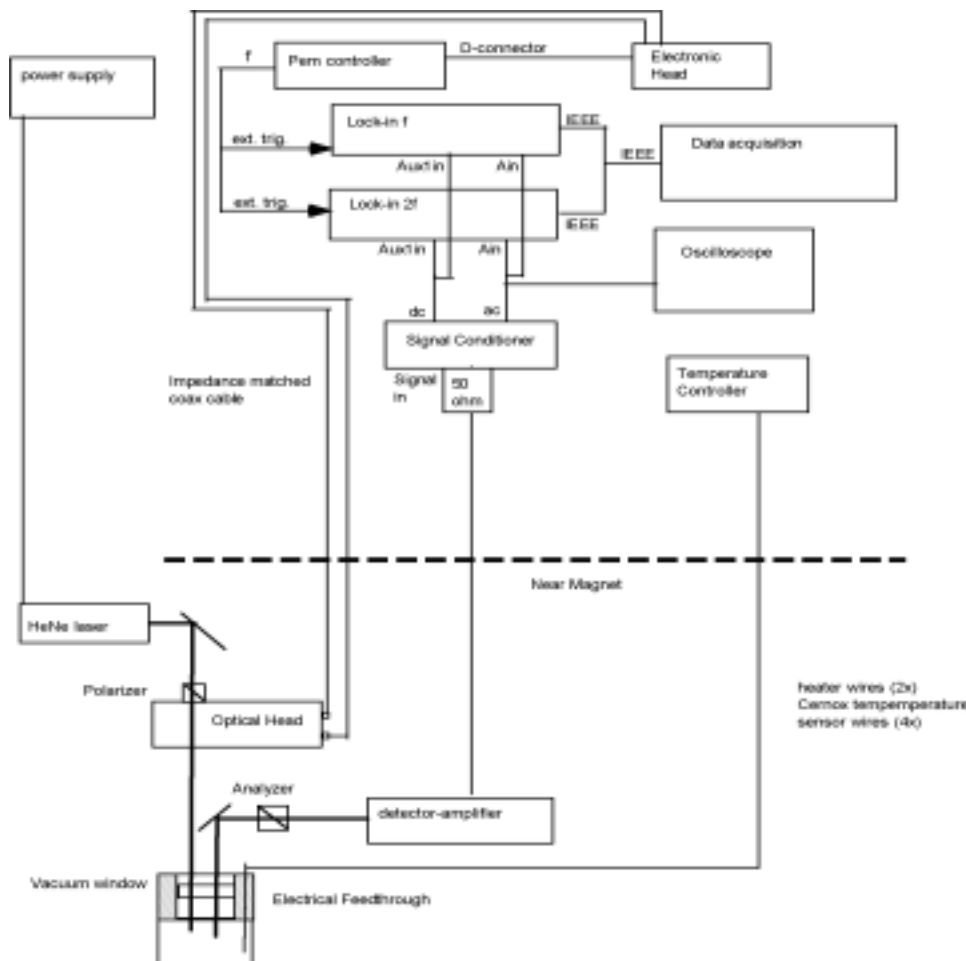


Figure1.7:Electronic setup

1.2 Data acquisition system.

The data acquisition is done by the standard LabView data-acquisition program. This program is basically an XY-writer written in LabView which runs on the Macintosh computer available at the NHMFL. The program can be found under “apple/labView/NML data acquisition. The program will start two different windows. One in which you can enter all the equipment and their addresses which are connected to the GPIB interface of the computer. The other window shows the data in graph form and gives all kind of options. Most of it is explained in Fig. 1.8.

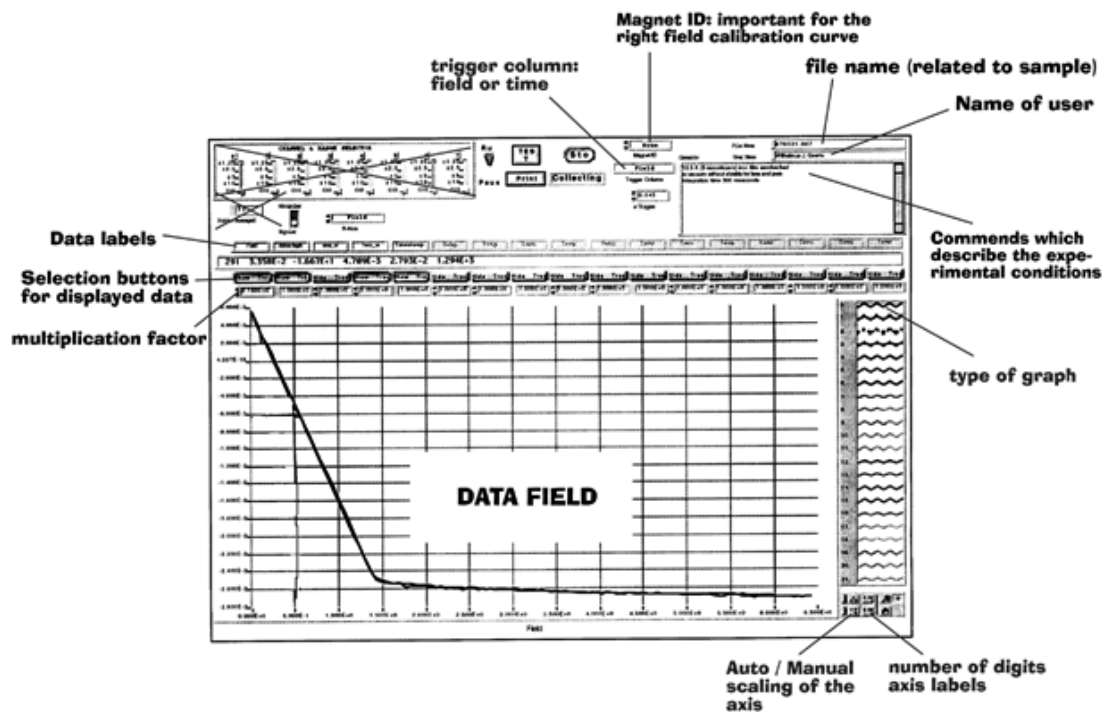


Figure1.8: Data acquisition system showing the ellipticity-field relation for 9 monolayers of epitaxial (001) iron sandwiched between gold.

1.4 Cryogenics.

The normal cryostats used for the resistive magnets consist of the Helium reservoir (inner bucket), the nitrogen reservoir (outer bucket), and a tail (see Fig. 1.9).

The nitrogen reservoir is completely isolated from the surroundings and the Helium reservoir by a double-sided wall separated by vacuum. Before starting the experiment one should assure oneself that this isolation vacuum is still sufficient. Pumping for _ to 1 hour on it should be sufficient. The tail contains an aluminum shield also isolated from the inside and outside of the tail by a vacuum and fishing-wire. The aluminum shield is thermally connected to the liquid nitrogen bath.

Before starting the cool-down procedure one should check if the vacuum jacket fits in the cryostat. The vacuum-can constrictor on the tail of the vacuum jacket has to be adjusted so that the sample will be at maximum field (see the markings, cell 3 respectively cell 5, on the tail of the cryostat

First step is to clean the Helium reservoir and tail of the cryostat. Any water or dirt should be removed. A special cleaning stick is available near the Kerr probe. After this, one should close the ports of the liquid helium reservoir, evacuate the reservoir, and refill it with helium gas (repeat this action two times).

Leave the cryostat connected to the helium gas bottles with a slight (~0.5 psi) over pressure.

Next step is to fill the outer bucket of the cryostat with liquid nitrogen. It will take approximately 1.5 hours to cool down the cryostat to 70 Kelvin. In the meantime we can cool the probe down to liquid nitrogen temperature in one of the pre-coolers available at the NHMFL. The pre-cooler is an isolated tube

(OD=4") of 2 meter which can be filled with

liquid nitrogen. Cooling down is best done with a small quantity of Helium exchange gas inside. Please be sure to purge the lines several times with helium gas because any air which enters the system will condense on the sample and distort your measurement results (the Kerr rotation of water is 4.4 mdegree/ μm in 20 tesla). Furthermore the ice crystals will scatter the light and decrease the measured values drastically.

When the cryostat is cooled down, the inner bucket can be filled with liquid helium. This filling should be done via the small tubes, and care should be taken not to let any air inside. Another 10 minutes should be waited to let the tail of the cryostat cool down till liquid helium temperatures.

When loading the probe into the cryostat special care should be taken not to let any air into the cryostat. The probe should be lifted with the crane and lowered till just above the cryostat. At that moment another person should remove the clamp and end cap (not the cryostat O-ring) of the helium reservoir and immediately place a rag over it. The probe should be lowered slowly (15 minutes) into the cryostat while wiping the frozen air of

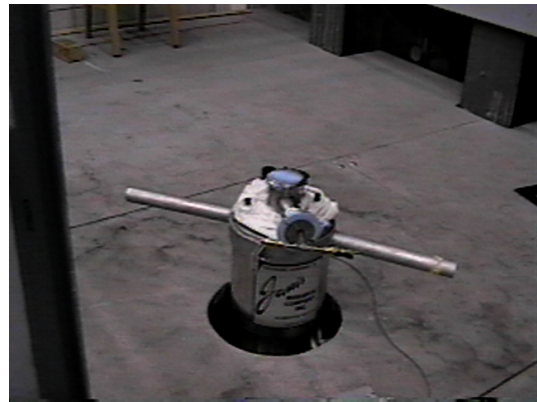


Figure 1.9: Cryostat

the vacuum can tail and keeping air from getting into the liquid helium reservoir. The holes in the constrictor should be opened up with an allen wrench before lowering it into the cryostat. After completion the liquid helium bath can be closed up with the ladish-quik-connect combination around the tube of the vacuum jacket. Be careful not to freeze the cryostat O-ring as it will not work in a frozen state. Before proceeding one should pump down the probe for ten minutes to remove the helium exchange gas. This will reduce the liquid helium consumption, reduce the Kerr rotation background, and improve the temperature control.

The temperature can be measured via a Cernox temperature sensor. Its leads are connected to the Detoronix connector at the top of lower course.

The range of the temperature control depends on the type of rings (Fig. 1.1) used in the sample stage. With the copper rings the temperature can be controlled from 2-160 Kelvin. With the G10 rings the higher temperature interval can be accessed (50-325 Kelvin).

1.5 Vacuum and Magnetic Shielding.

The Kerr rotation from the air in the vacuum jacket is approximately 440 mdegrees (over 20 tesla) for the magnet of cell 3. For measurements in the mdegree range it is therefore necessary to evacuate the probe. At NHMFL several pump combinations are available. If one decides to put a pump on the magnet platform, one should realize that it is better not to use a turbo-pump when the magnet is on. This in order to avoid that the blades will crash.

Most of the optics, including. lens, vacuum window, modulator, analyzer and polarizer, is shielded. The materials used to shield are magnetic iron and μ -metal. One should realize that the forces on these magnetic materials can be quite large. The weight of the lens shield will increase by more than a factor of five when ramping up the field to 20 tesla.

For this reason one should not remove the probe, or any of the shielded objects when the magnet is on.

This is in order to avoid dangerous situations. Always check to be sure the probe is tightly secured in the cryostat before ramping up the magnetic field.

Although the shields have only a small effect at 633 nm, their presence is crucial at the shorter wavelengths.

2. Background Information.

2.1 Measurement technique [4].

In this section the mathematical background of the used measurement technique is presented. Consider the optical setup of Fig. 0.4. The phase shift introduced by the PEM, δ , can be described by:

$$\delta = \delta_0 \sin(2\pi p t)$$

Where δ_0 is the modulation depth, p is the modulation frequency of the PEM (=50 kHz), and t is the time.

Then the intensity of the light on the detector can be described by:

$$I = \frac{\epsilon E^2}{4\pi} R + \frac{\Delta R}{2} \sin(\delta) + R \sin(\Delta\theta + 2\varphi) \cos \delta$$

where E depends on the laser intensity, φ the angle between the analyzer and the modulation direction of the PEM, and the parameters R , ΔR and $\Delta\theta$ properties of the sample which are defined as:

$$R = \frac{1}{2}(r_+^2 + r_-^2), \Delta R = r_+^2 - r_-^2, \Delta\theta = \theta_+ - \theta_-$$

and r_{\pm} and θ_{\pm} are related to the Fresnel coefficients $r_{\pm} e^{i\theta_{\pm}}$. We have assumed that $\Delta R/R \ll 1$.

The MO parameters (Kerr rotation, θ_k , and Kerr Ellipticity, η_k) can than be expressed as:

$$\theta_k = \frac{\Delta\theta}{2}, \eta_k = \frac{\Delta R}{4R}$$

The intensity of the light at the detector can be written as:

$$I = I(0) + I(p) \sin(2\pi p t) + I(2p) \sin(4\pi p t) +$$

where:

$$I(0) = I_0 R [1 + J_0(\delta_0) \sin(\Delta\theta + 2\varphi)]$$

$$I(p) = I_0 \Delta R J_1(\delta_0)$$

$$I(2p) = 2I_0 R J_2(\delta_0) \sin(\Delta\theta + 2\varphi)$$

where δ_0 is the retardation amplitude (in rad), $\Delta\theta$ is the phase shift upon reflection between the LCP and the RCP incoming light, $I_0 = (\epsilon/8\pi)E^2$ and J_0 , J_1 and J_2 are the 0th, 1st, and 2nd order Bessel functions, respectively. Fig. 2.1 shows a graph with these functions for arguments smaller than 10.

Assuming that the amplification factor for the ω and the 2ω component are the same we may write:

$$\frac{I(p)}{I(0)} = BJ_1(\delta_0) \frac{\Delta R}{R} = 4BJ_1(\delta_0)\eta_k$$

$$\frac{I(2p)}{I(0)} = BJ_2(\delta_0)2\Delta\theta = -BJ_2(\delta_0)\theta_k$$

where B is the ratio between the AC and the DC amplification of the silicon detector amplifier and the signal conditioner.

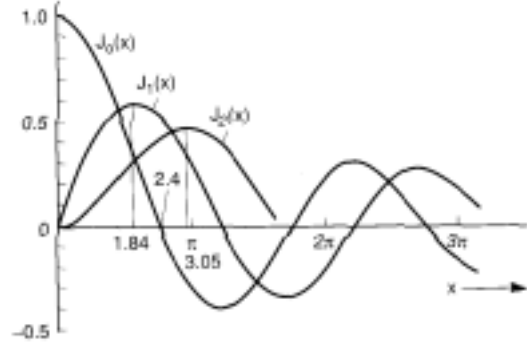


Figure 2.1: The Bessel functions $J_0(x)$, $J_1(x)$, and $J_2(x)$.

2.2 Calibration

Calibration of the system can be obtained in three different ways:

- Measuring a standard sample from which the effects are exactly known.
- Measuring the Kerr rotation background with 1 atmosphere nitrogen gas in the probe. One should not use air as water will condense on the sample surface, even if the probe is not cooled. The nitrogen background for cell 3 was about 22 mdegree/tesla. This technique will not work at low temperatures.
- The 2ω signal has the same sensitivity for the Kerr rotation signal as for the angle of the analyzer. From accurate measurements of the 2ω as a function of the analyzer angle at -4, -2, 0, 2, and 4 degrees one can calculate the calibration factor for the Kerr rotation signal.

The calibration factor for the rotation (A_{rot}) and ellipticity (A_{ell}) are related with each other via the following equation:

$$A_{rot} = -4 * A_{ell} * \frac{J_1(\delta_0)}{J_2(\delta_0)}$$

In which J_1 and J_2 are the first and second Bessel functions (see Fig. 2.2.1) and δ_0 is the modulation depth of the PEM. Table 2 gives some values of A_{rot}/A_{ell} for different values of the δ_0 .

Table 2: Estimated calibration ratios for different modulation depths.

δ_0	description	A_{rot}	$A_{\text{rot}}/A_{\text{cll}}$
$\pi/2$	maximum 1ω sensitivity	0.3	0.5
2.4	real DC signal	0.4	0.3
2.6	$J_1(\delta_0) = J_2(\delta_0)$	0.45	0.25
π	maximum 2ω sensitivity	0.5	0.2

The third column of Table 2 gives the A_{rot} for the case the ratio of the DC amplification and the AC amplification is equal to 1. The amplification factors of both signals can be set by set-screws in the signal conditioning unit of HINDS.

2.1 Specifications MOK3

light source:	linear polarized HeNe laser 632 nm (1.96 eV), 2 mW.
polarizer/analyzer:	Glan-Thompson, Glan-Laser
noise (100 nm Fe film):	smaller than 0.5 mdegree
reloading time:	room temperature: 15 minutes liquid helium temperature: 2 hours
background in vacuum:	ellipticity signal: assymetric 0.5 to 1 mdegree/tesla rotation signal \ll 2 mdegree/tesla
measurement mode:	polar Kerr, longitudinal Kerr, polar Faraday
sample space:	2 cm diameter, 2.5 cm height (with heater) 2 cm diameter, 3 cm height (without heater)
Liquid / Gas cells:	Hellma Cell Inc.: 718-544-9534, David Friedmann
Pressure cells:	Diamond anvil cell: ask Stan Tozer
Data acquisition:	Data acquisition NML © Scott Hannahs
beam diameter:	2 mm
temperature range:	2-160 Kelvin (with copper rings) 50-325 Kelvin (with G10 rings)
heater:	50 ohm, 5 Watt
temperature sensor:	Cernox number x01974
electrical feedthrough:	19 pins Detoronix

Trouble shooting list: UNDER CONSTRUCTION

References.

- [1] J. Kerr, "On the rotation of the plane of polarization by reflection from the pole of a magnet", *Phil. Mag.* 3 (1877) 339-343.
- [2] M. Faraday, "On the magnetization of light and the illumination of magnetic lines of force", *Trans. Roy. Soc. London* 5 (1846) 592.
- [3] W. Bas Zeper, "Magneto-Optical recording media based on Co/Pt multilayers", Ph.D. Thesis University of Twente, The Netherlands (1991).
- [4] William van Drent, "CoNi/Pt multilayers for magneto-optical recording", Ph.D. Thesis University of Twente, The Netherlands (1995).
- [5] Wim Geerts, "Magnetization distribution at the surface of Co-Cr films: Magneto-Optical, Chemical, and Structural Characterization.", Ph.D. Thesis University of Twente, The Netherlands (1992).
- [6] M.J. Freiser, "A survey on magneto-optics", *IEEE Trans. Magn.* 4 (1968) 152-161.
- [7] H.S. Bennet, E. Stern, "Faraday effects in solids", *Phys. Rev. A* 137 (1965) A448-461.
- [8] H.R. Hulme, "The Faraday effects in ferromagnetics", *Proc. R. Soc. Lond.* 135 (1932) 237.
- [9] L. Berger, *Phys. Rev. B* 2 (1970) 4559.
- [10] J.L. Erskine, E.A. Stern, "Magneto-Optical Kerr effects in Gadolinium", *Phys. Rev. B* 8 (1973) 1239-1255
- [11] S.N. Jasperson and S.E. Schnatterly, "An improved method for high reflectivity ellipsometry based on a new polarization modulation technique", *Rev. Sci. Instrum.* 40 (1969) 761.
- [12] K. Sato, "Measurement of Magneto-Optical Kerr effects using Piezo-Birefringent Modulator, *Jap. J. Appl. Phys.* 20 91981) 2403.
- [13] Theodore C. Oakberg, "Modulated Interference effects: Use of photoelastic modulators with lasers", 1994, Manual of the HINDS PEM.

List of Figures:

Fig. 0.1: Definition of Kerr rotation and Kerr ellipticity

Fig. 0.2: The three Kerr configurations: (a) Polar, (b) Longitudinal, and (c) Transverse.

Fig. 0.3: Microscopic origin of the Magneto-Optical effects: Simplified energy-level scheme for a transition: (a) fully degenerate, (b) including exchange splitting, (c) including spin orbit interaction, (d) in a material with a bandstructure [3].

Fig. 0.4: Global measurement scheme.

Fig. 0.5: (a) Retardation of the PEM as a function of the time, (b) polarization state of corresponding light vector, (c) as (b) but after introduction of Kerr rotation, (d) as (b) but after introduction of Kerr ellipticity signal [12].

Fig. 1.1: Lower course of the probe.

Fig. 1.2: (a) sample stage close up, (b) Faraday adapter, (c) longitudinal adapter.

Fig. 1.3: Upper course in probe holder.

Fig. 1.4: center unit.

Fig. 1.5: (a) alignment strategy for polar configuration, (b) alignment strategy for longitudinal configuration.

Fig. 1.6: alignment elbow

Fig. 1.7: Electronic setup

Fig. 1.8: Data acquisition system

Fig. 1.9: Cryostat

Fig. 2.1: First three Bessel functions.